

Patient ID	1-II:1	2-II:1	3-III:1	4-I:2	4-II:1	4-II:3	4-III:1	5-II:2	5-III:1	5-III:2	6-II:6	6-III:5	6-III:6	7-III:1	8-II:3
Mutation	del	del	p.R330C	p.P366H				p.R327W			p.Y369Cfs*26			p.A100_Y104 del	p.Y99*
Sex	M	M	F	M	M	M	M	M	F	M	M	M	M	F	M
Age	46	9	13	61	32	32	3	44	21	7	43	10	7	28	50
Craniofacial															
Eye	myopia	hyperopia	lens opacities	myopia	excav. papil	myopia	nl	retinal detach	nl	nl	astigm	nl	nl	nl	myopia
Downslant palpebral fissures	-	+	+	-	+	+	-	+	+	-	+	+	+	+	-
Hypertelorism	+	-	+	-	-	-	-	-	-	-	+	+	-	+	-
High arched palate	+	+	+	+	+	+	+	+	+	-	-	+	-	-	-
Uvula	nl	nl	nl	nl	nl	nl	nl	broad	nl	nl	nl	nl	nl	broad	bifid
Retrognathia	+	+	+	+	+	+	+	+	-	+	+	-	-	+	-
Other	torticollis	ptosis					ptosis			torticollis plagiocep.				spondylosis subluxation C7 over T1	
Skeletal															
Stature (cm or percentile if child)	193	P95	P9	171	200	196	>P95	184	173	P95	196	P95	P95	177	167
Armspan ratio	1.02	0.96		1.08			0.95	1.04	1.01	1.02				1.03	
Pectus Deformity	+	+	+	+	+	+	+	-	-	-	-	-	+	+	-
Scoliosis	+	-	-	+	+	+	-	-	-	-	-	-	-	-	+
Arachnodactyly	+	+	+	+	+	+	-	+	-	-	-	-	-	+	-
Club feet	+	+	+	-	-	-	-	+	-	-	-	-	-	+	-
Pes planus	-	+	-	+	+	+	+	+	+	-	-	-	-	+	-
Hypermobility (Beighton > 5/9)	-	-	+	+	+	+	+	-	-	-	-	-	-	+	+
Other	Claw toes	Claw toes						Knee dislocation							
Cardiovascular															
Aortic root Z-score	2.8	3	+	2	2.4	4.3	3	4*	3.7	6	3.4	2.4	2.6	7*	8.4*
Ao dissection/repair	Type B age 42							VSARR (45 mm)						VSARR (48 mm)	VSARR (56 mm)
Aortic valve	TAV	TAV	TAV	TAV	TAV	TAV	TAV	AVR	TAV	TAV	TAV	BAV	BAV	TAV	TAV
Mitral valve	MVP	-	-	MV-S	MVP	MVP		MV-S	MVP with MR	MR					-

Other	VSD										MPA			Tortuosity ASD	SVT
Skin															
Striae	-	-	-	-	+	+	-	-	-	-	+	-	-	-	-
Hernia	+	-	+	+	+	+	-	+	+	+	+	-	-	-	+
Easy bruising	-	-	+	-			-	+	+	+	+			-	-
Other			Thin	Varicose veins			Thin	Thin Dystrophic scars	soft	soft	soft	Keloid scars			Levold reticularis
Dura	ND	ND	ND	Tarlov cyst	Tarlov cyst	-	ND	ND			Tarlov cyst			Dural ectasia	-
Other findings	Cryptorchidism	Hypotonia, ataxia									Supernumerary nipple				

Supplementary Table 1: Abbreviations: VSARR: valve sparing aortic root replacement; BAV, bicuspid aortic valve; TAV, tricuspid aortic valve; MVP, mitral valve prolapse; MV-S: mitral valve surgery; ASD, atrial septal defect (surgically closed at time of VSARR); VSD, ventricular septal defect; MPA, main pulmonary artery aneurysm; SVT supraventricular tachycardia; ND not done; * Z-score at time of surgery

Supplementary Table 2: TGFB2 primers and PCR conditions

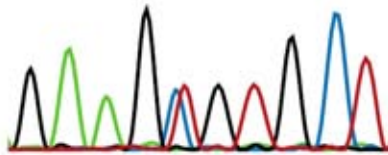
Name	Forward	Reverse	Length	Protocol ¹
TGFB2-Exon1	AGGGTTCCTCTGCCCCGTCC	CCGGGAGCTGCTGCGGTTTT	670	1
TGFB2-Exon2	ATCCCCTGGCCCCAGGTAGC	TCGCTCAGGTACAAGGCTGCAT	365	1
TGFB2-Exon3	TTCCACCAGTCTGTCAGCCTCAA	TCGGGTGTGATGGTGCACTCC	645	2
TGFB2-Exon4-5	TTCATGGCAAATAGCCTGGTGTGT	TAGACCCTTCCCTCCCCACCT	596	1
TGFB2-Exon6	AGCCCTGGCTTTGACACCGA	TCTGGCCTTAGCAGTGAGTTCCAC	534	2
TGFB2-Exon7	TGGTTTGGGGTGAGGTGGTGG	TGTGATGGTAAGACAGCACGAGGT	344	2
TGFB2-Exon8	TGCCTACTCAGTGCTGTGACTGCT	AGGCGCGGGATAGGAACGGT	666	2

¹: *Protocol 1*: 94°C 5min - [94°C 15s - 60°C 30s - 72°C 45s]x34 - 72°C 10min; *Protocol 2*: 94°C 3min - [94°C 30s - 67°C 30s (-0,5°C per cyclus) - 72°C 45s]x14 -

[94°C 30s - 60°C 30s - 72°C 45s]x20 - 72°C 10min

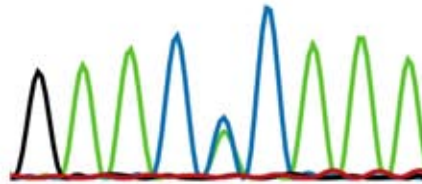
Supplementary Figure 1

c.988 C>T; CGT>TGT
p.Arg330Cys



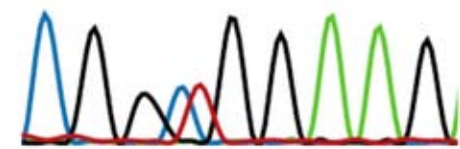
Family 3

c.1097 C>A; CCC>CAC
p.Pro366His



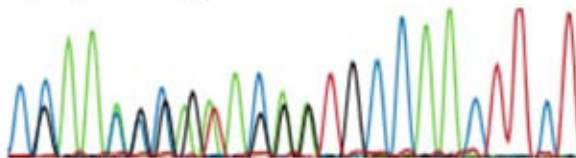
Family 4

c.979 C>T; CGG>TGG
p.Arg327Trp



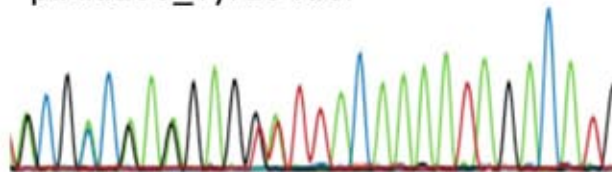
Family 5

c.1106_1110delACAAT
p.Tyr369Cysfs*26



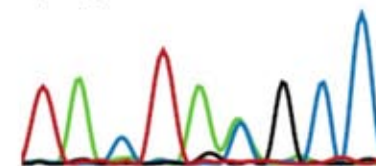
Family 6

c.294_308 delCTACGCCAAGGAGGT
p.Ala100_Tyr104del



Family 7

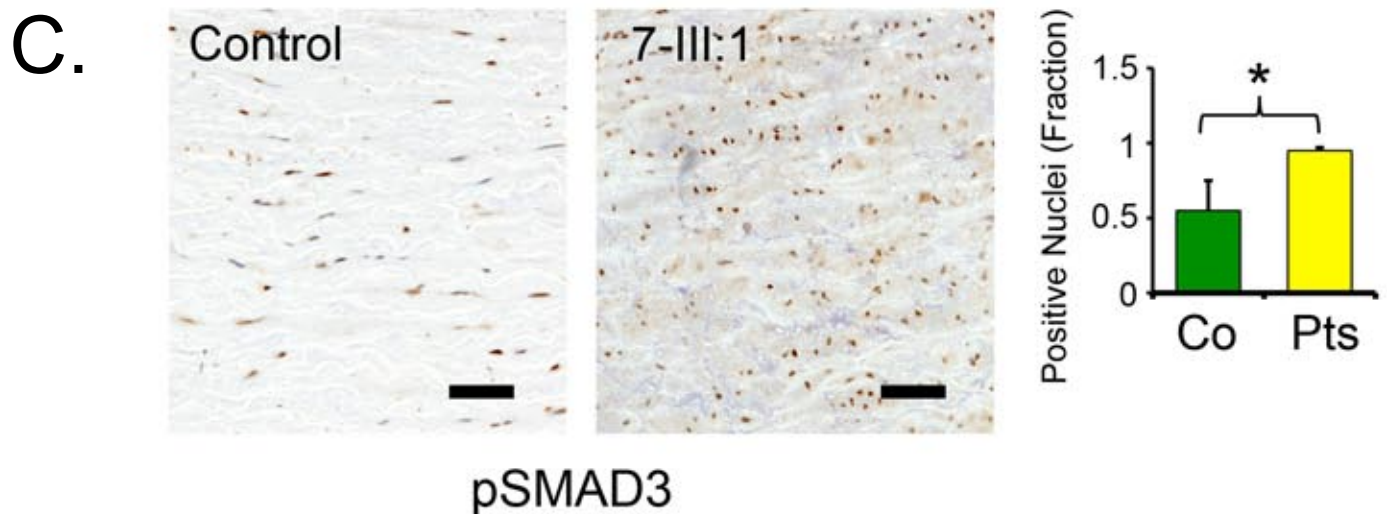
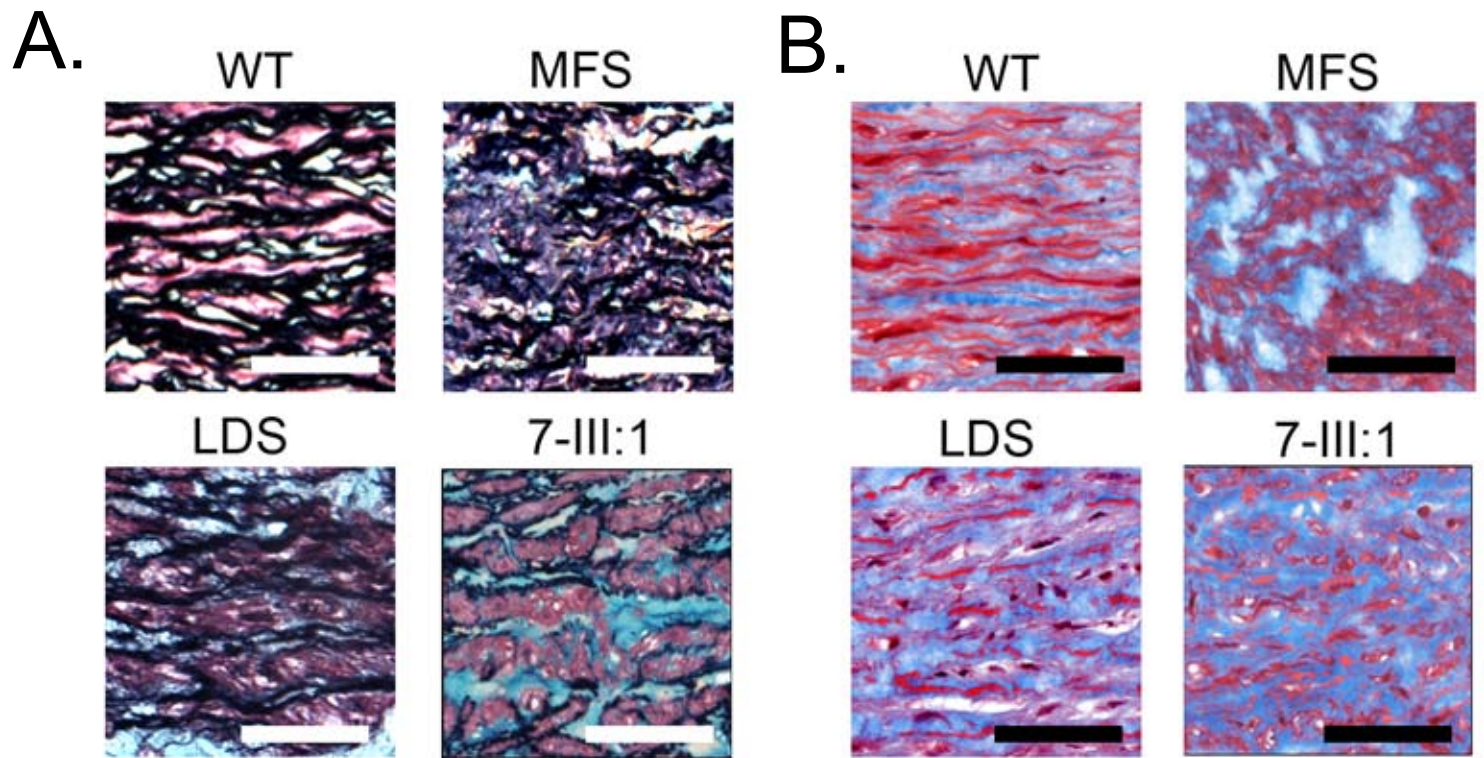
c.297C>A; TAC>TAA
p.Tyr99*



Family 8

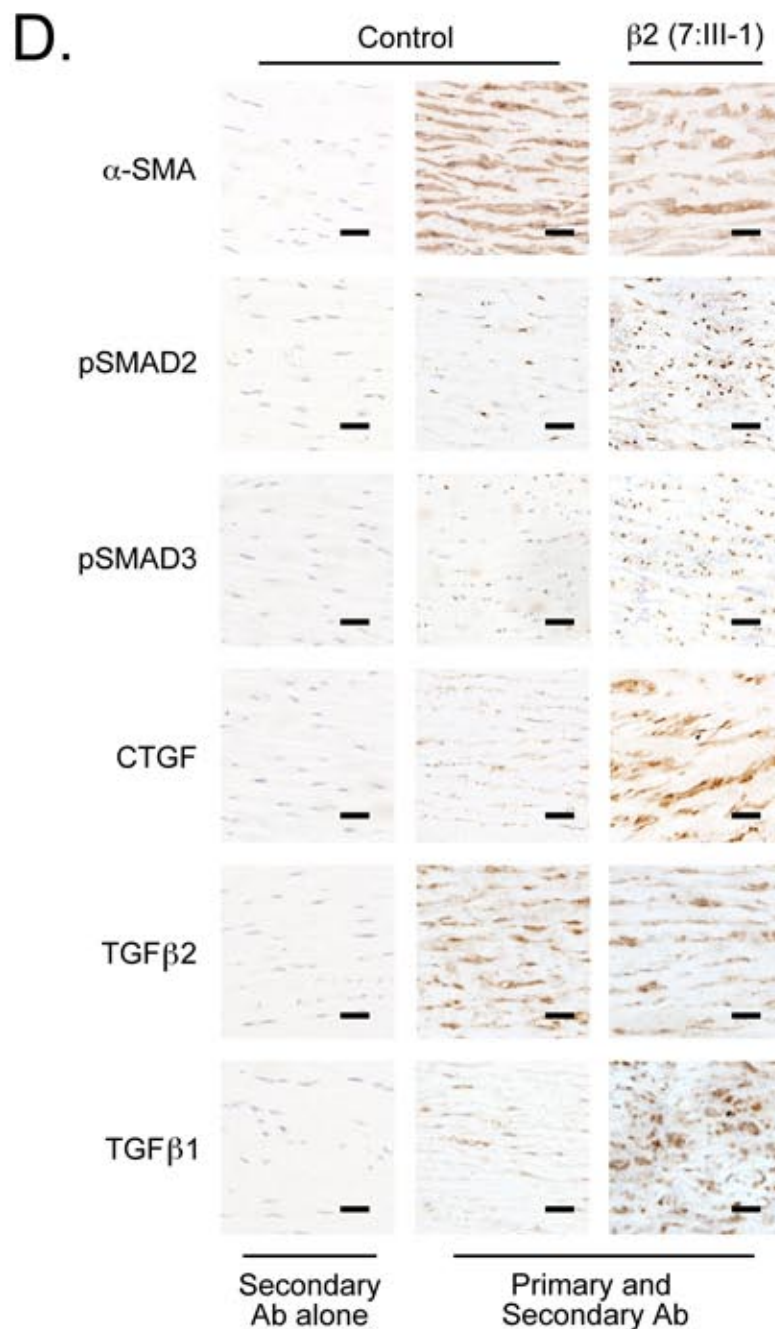
Supplemental Figure 1 : Sequence chromatograms and corresponding interpretation of familial *TGFB2* mutations are displayed (Family 3 through Family 8).

Supplementary Figure 2



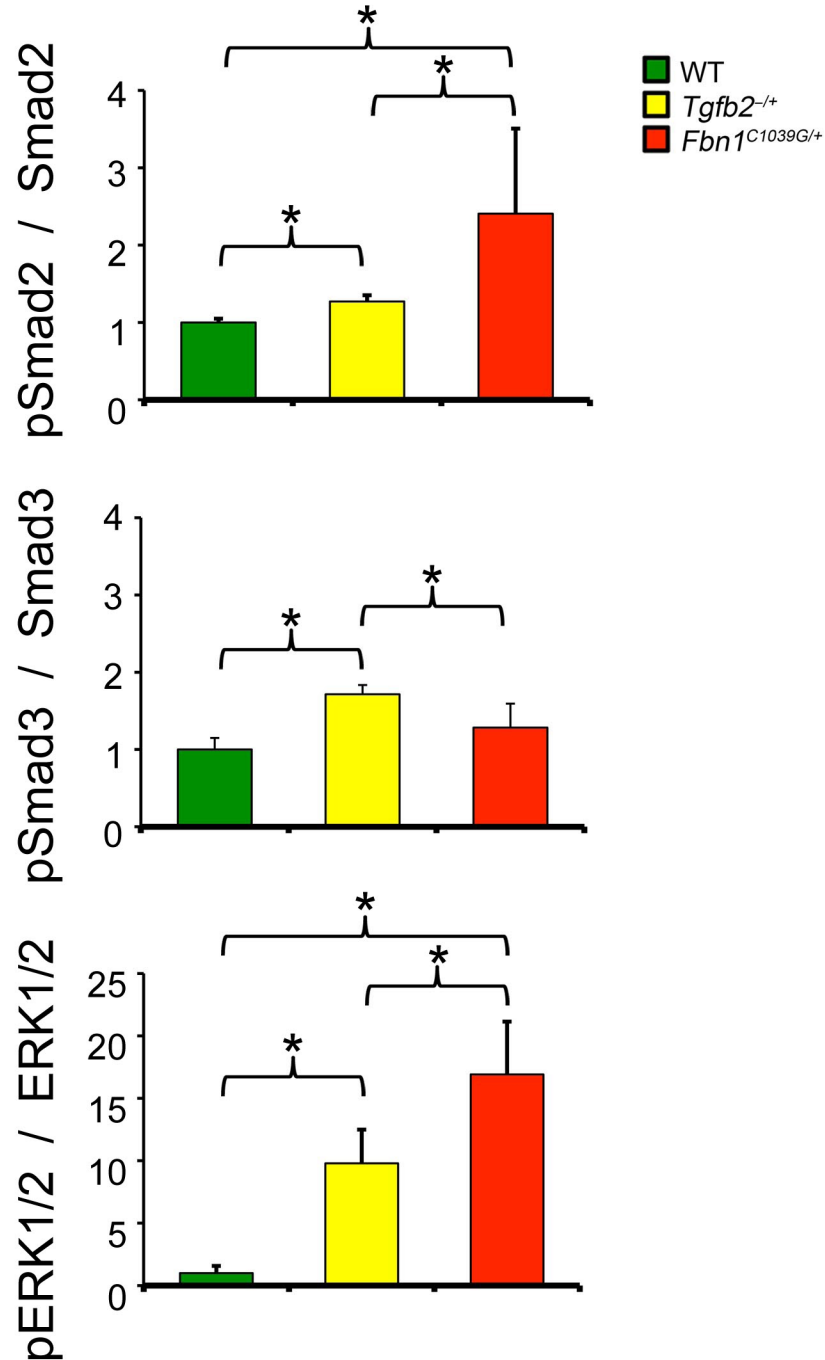
Supplemental Figure 2 : (A.) High magnification view of Movat's pentachrome staining of human aortic samples demonstrating an increase in proteoglycan deposition (Blue staining in Movat's pentachrome) and elastic fragmentation (Black in Movat's pentachrome) in MFS, LDS, and patient with *TGFB2* mutation (7:III-1) versus control, Bar= 80 μ M. (B.) High magnification view of Masson's Trichrome staining of human aortic samples with increased collagen deposition (Blue in Masson's Trichrome) in MFS, LDS, and patient with *TGFB2* mutation (7:III-1) versus control, Bar= 80 μ M. (C.) Quantification of fraction of pSMAD3 positive nuclei of control aortas (3) versus patients (7:III-1 and 5:II-2), (* p <0.05), Error bars equal 2 SEM, Bar= 80 μ M.

Supplementary Figure 2



Supplementary Figure 2: (D.) Staining controls for human aortic IHC. Column 1 represents secondary antibody staining controls. Second and third columns represent staining with indicated primary and secondary antibodies of either control aorta (Column 2) or mutant aorta (Column 3). Bar= 80 μ M.

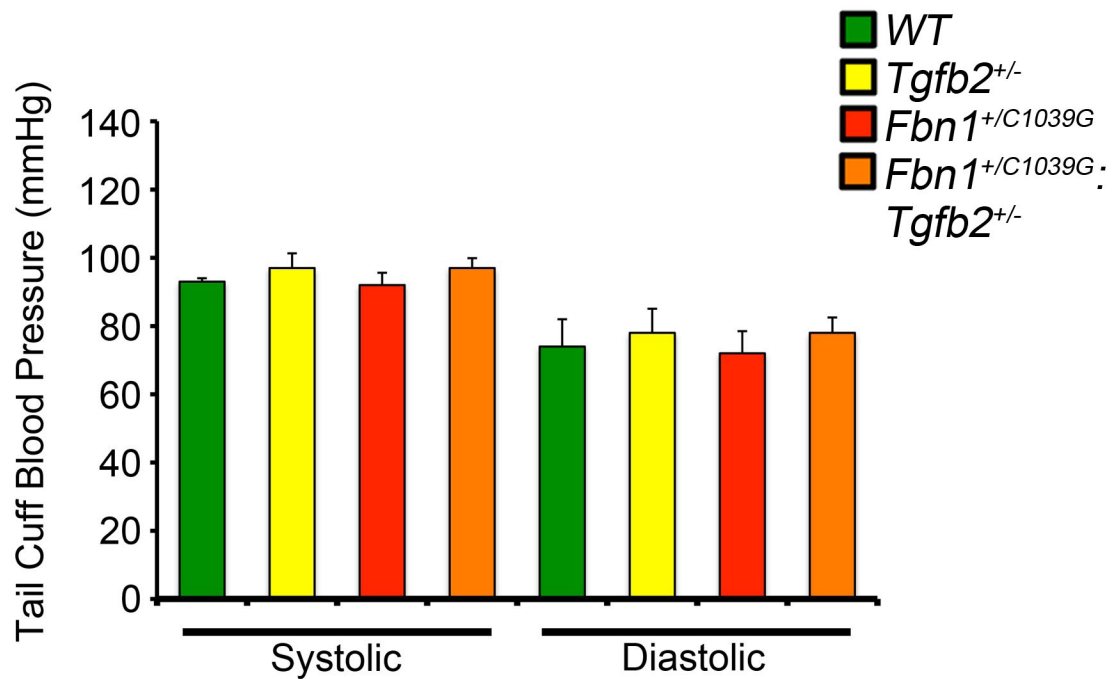
Supplementary Figure 3



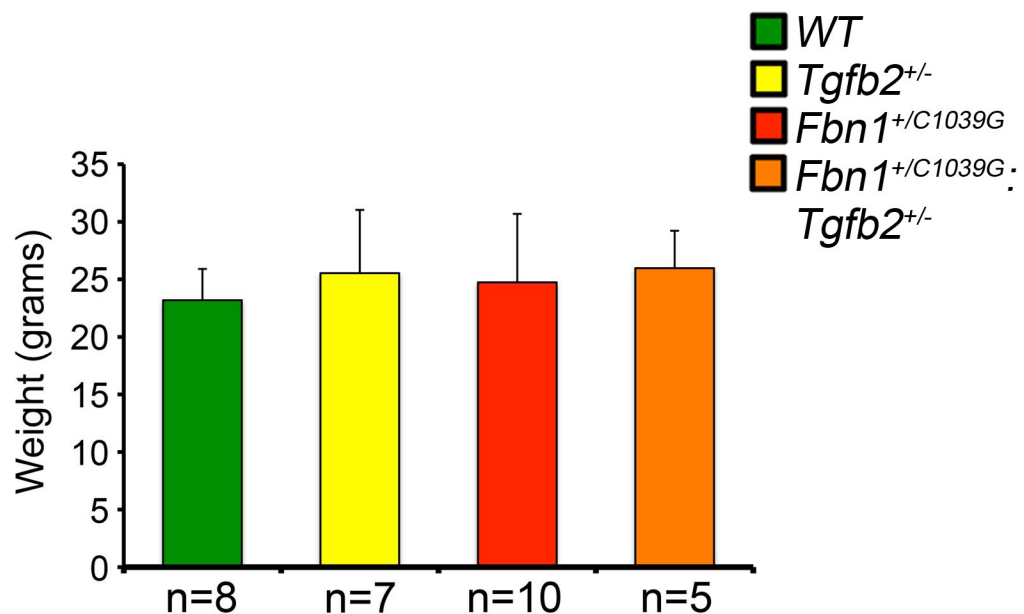
Supplemental Figure 3: Ratio of phosphorylated Smad2 western blot staining to total Smad2 and phosphorylated ERK1/2 western blot staining to total ERK1/2 western blot staining for 8 month old of WT, *Tgfb2*^{+/-}, or *Fbn1*^{+/*C1039G*} aortas, Error bars equal 2 SEM, (n=4 for each genotype), (*p<0.05).

Supplementary Figure 4

A.

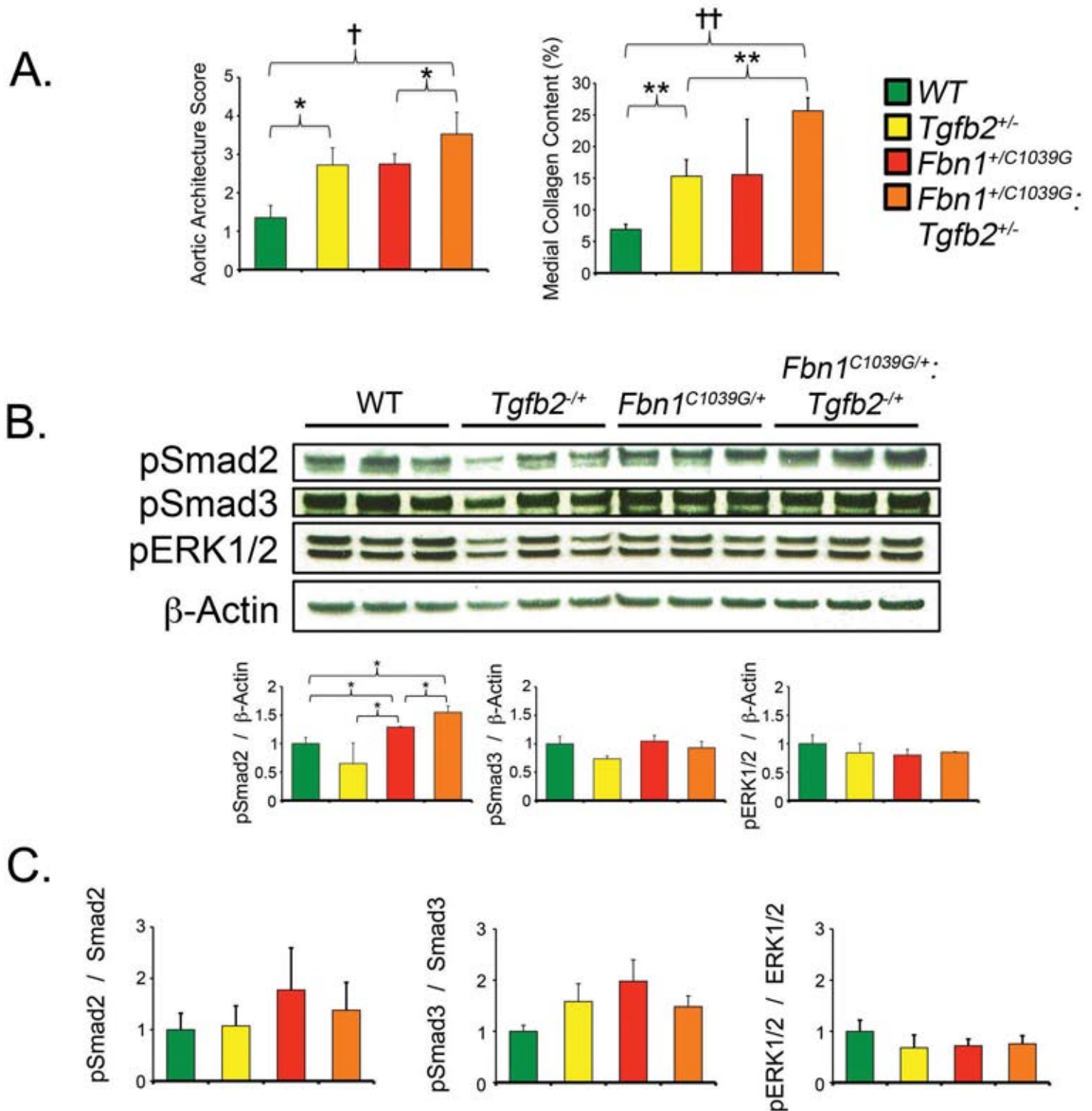


B.



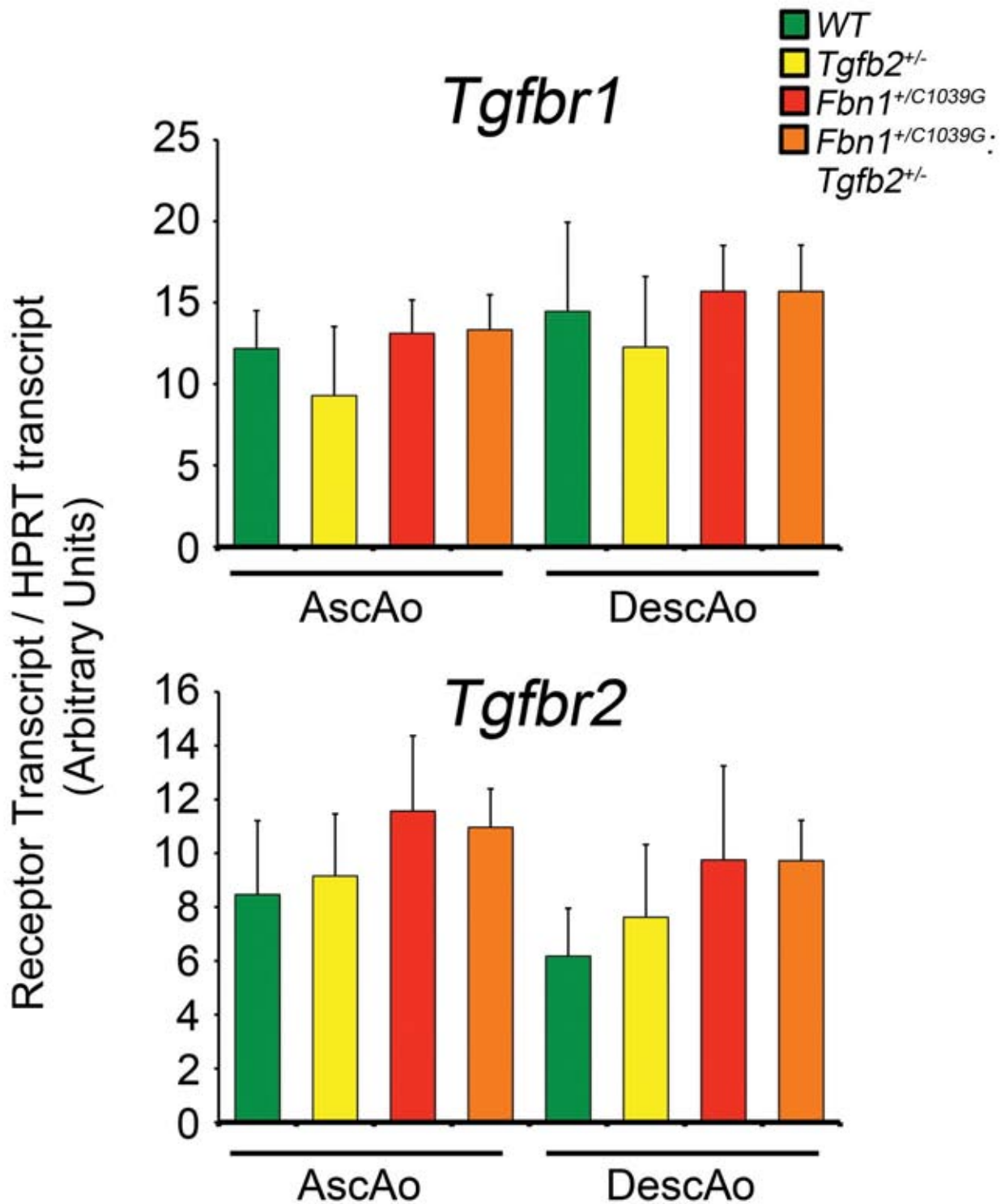
Supplemental Figure 4: Normal hemodynamic measurements and body size in *Tgfb2*^{+/-}; *Fbn1*^{+/*C1039G*} synthetic mice. (A.) Blood pressure quantification (systolic and diastolic) of WT, *Tgfb2*^{+/-}, *Fbn1*^{+/*C1039G*}, and *Tgfb2*^{+/-}; *Fbn1*^{+/*C1039G*} mice by tail cuff measurement. (B.) Weight of 4 month old WT, *Tgfb2*^{+/-}, *Fbn1*^{+/*C1039G*}, and *Tgfb2*^{+/-}; *Fbn1*^{+/*C1039G*} mice demonstrate no significant differences, Error bars equal 2 SEM.

Supplementary Figure 5



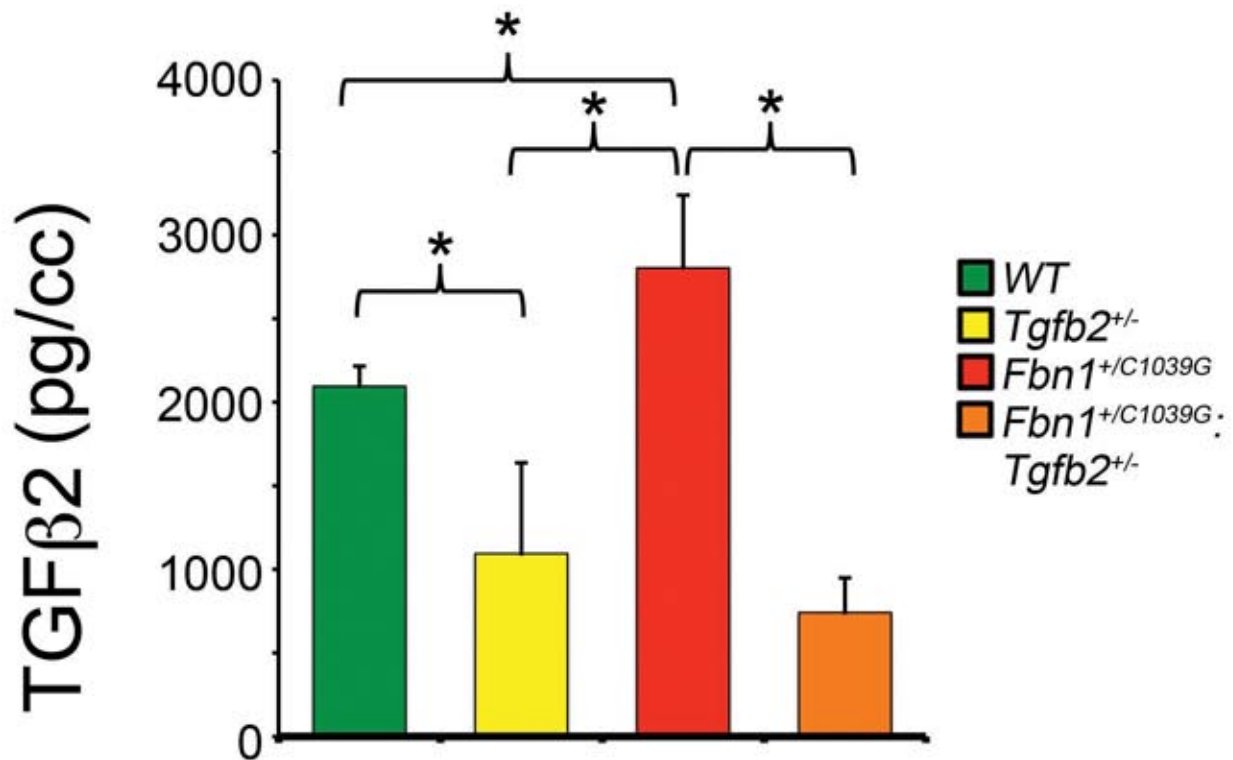
Supplemental Figure 5: (A.) Quantification of Aortic Histology in *Tgfb2*^{+/-}; *Fbn1*^{+/*C1039G*} synthetic mice. Graphs represent quantification of aortic architecture score and aortic collagen deposition, Error bars equal 2 SEM, (*p<0.05, **p<0.01, †p<0.005, ††p<0.001). (B.) Signaling within *Tgfb2*^{+/-}; *Fbn1*^{+/*C1039G*} aortas. Western blotting of aortas demonstrating increased phosphorylation of Smad2 in WT, *Tgfb2*^{+/-}, *Fbn1*^{*C1039G*/+}, and *Tgfb2*^{+/-}; *Fbn1*^{+/*C1039G*} mice. Quantification graphs of western blots (*p<0.05) Error bars equal 2 SEM. (C.) Ratio of phosphorylated Smad2 western blot staining to total Smad2 and phosphorylated ERK1/2 western blot staining to total ERK1/2 western blot staining for 4 month old of WT, *Tgfb2*^{+/-}, *Fbn1*^{+/*C1039G*} and *Tgfb2*^{+/-}; *Fbn1*^{+/*C1039G*} murine aortas, (n=3 for each genotype), Error bars equal 2 SEM.

Supplementary Figure 6



Supplemental Figure 6: Transcript analysis of *Tgfbr1* and *Tgfbr2* in ascending and descending aortas of 2 month old WT (n=3), *Tgfb2*^{+/-} (n=3), *Fbn1*^{+/*C1039G*} (n=3), and *Tgfb2*^{+/-}; *Fbn1*^{+/*C1039G*} (n=3) mice normalized to HPRT expression. There were no statistically significant differences, Error bars equal 2 SEM.

Supplementary Figure 7



Supplemental Figure 7: Analysis of circulating TGFβ2 levels in mouse plasma from 4 month old WT (n=4), Tgfb2^{+/-} (n=4), Fbn1^{+/-}C1039G (n=4), and Tgfb2^{+/-}; Fbn1^{+/-}C1039G (n=4) animals. Ligand levels are expressed in units of picogram per milliliter. (*p<0.05). Error bars equal 2 SEM.